Phonon density of states of single-crystal $SrFe_2As_2$ across the collapsed phase transition at high pressure

Y. Q. Wang,[1] P. C. Lu,[2] J. J. Wu,[3,4] J. Liu,[5] X. C. Wang,[4] J. Y. Zhao,[6] W. Bi,[6,7] E. E. Alp,[6]
C. Y. Park,[8] D. Popov,[8] C. Q. Jin ,[4] J. Sun,[2,9,*] and J. F. Lin[3,5,†]

[1]*School of Physics and Electronics Engineering, Zhengzhou University of Light Industry, Zhengzhou 450002, China*
[2]*School of Physics and National Laboratory of Solid State Microstructures, Nanjing University, Nanjing 210093, China*
[3]*Center for High Pressure Science and Technology Advanced Research, Shanghai 201203, China*
[4]*Beijing National Laboratory for Condensed Matter Physics and Institute of Physics, Chinese Academy of Sciences, Beijing 100190, China*
[5]*Department of Geological Sciences, Jackson School of Geosciences, The University of Texas at Austin, Austin, Texas 78712, USA*
[6]*Advanced Photon Source, Argonne National Laboratory, Argonne, Illinois 60439, USA*
[7]*Department of Geology, University of Illinois at Urbana-Champaign, Urbana, Illinois 61801, USA*
[8]*HPCAT, Carnegie Institution of Washington, Advanced Photon Source, Argonne National Laboratory, Argonne, Illinois 60439, USA*
[9]*Collaborative Innovation Center of Advanced Microstructures, Nanjing University, Nanjing 210093, China*

(Received 27 March 2016; revised manuscript received 28 June 2016; published 25 July 2016)

To help our understanding of the structural and superconducting transitions in ferropnictides, partial phonon density of states (PDOS) of iron in a single-crystal $SrFe_2As_2$ pnictide have been investigated from both out-of-plane and in-plane polarizations with respect to the basal plane of the crystal structure using nuclear resonant inelastic x-ray scattering in a high-pressure diamond anvil cell at ambient temperature. The partial PDOS of iron in the pnictide crystal changes dramatically at approximately 8 GPa, which can be associated with the tetragonal (T) to collapsed tetragonal (CT) isostructural transition as evidenced in high-pressure x-ray diffraction measurements and theoretical calculations. Across the T-CT phase transition, analysis of the PDOS spectra shows a rapid stiffening of the optical phonon modes and a dramatic increase of the Lamb-Mössbauer factor (f_{LM}) and mean force constant which can be associated with the rapid decrease of the c axis and the anomalous expansion of the a axis. Theoretically calculated Fe partial PDOS and lattice parameters of $SrFe_2As_2$ further reveal the strong correlation between the lattice parameters and phonons. Our results show that the T-CT transition can induce significant changes in the vibrational, elastic, and thermodynamic properties of $SrFe_2As_2$ single crystal at high pressure.

DOI: 10.1103/PhysRevB.94.014516

I. INTRODUCTION

The discovery of the high-transition-temperature (T_c) superconductivity in ferropnictides has inspired renewed research interest in the fundamental physics of the origin of superconductivity [1]. Thus far, all of the newly discovered ferropnictide superconductors exhibit tetrahedral coordinated FeAs layers [2,3]. The parent ferropnictide compounds undergo a structural transition from a tetragonal to an orthorhombic phase at low temperatures that is accompanied by a paramagnetic (PM) to an antiferromagnetic (AFM) spin density wave (SDW) transition [4–6]. Superconductivity in this system can be induced by chemical doping or applied pressure to suppress the SDW [3,7]. The interplay of the structure and magnetism is believed to play an important role in the origin of superconductivity in the pnictide superconductors [2]. First-principles calculations have shown that the electron-phonon coupling is too weak to give rise to the high T_c in the ferropnictide superconductors [8]. However, many recent theoretical calculations and experimental results have indicated that the phonon coupling with the magnetism or the spin fluctuations in the compound can play an important role in the origin of the superconductivity [9,10]. In particular, a large isotope effect related to Coulomb interactions between electrons, in which the isotope coefficient is defined by $-d\ln T_c/d\ln M$, where M is the isotope mass, has been observed in $Ba_{1-x}K_xFe_2As_2$ and $SmFeAsO_{1-x}F_x$ iron pnictide superconductors [11]. A similar isotope effect was also reported for the FeSe compound [12], demonstrating that the phonon-electron coupling in iron pnictides cannot be ruled out as a fundamental mechanism for the origin of superconductivity in pnictides.

Superconductivity can also be induced by applying pressure to the parent pnictide compounds [3,7]. Compared to chemical doping, applied pressure introduces less disorder and was found to be a powerful tool to unravel the intrinsic properties in the iron pnictides [13]. Previous high-pressure studies performed on $BaFe_2As_2$ reveal that the structural and antiferromagnetic transitions are rapidly suppressed by applied pressure before the superconductivity of the system occurs, although some crucial issues remain to be addressed, including the effects of hydrostaticity and uniaxial stress on the structural, magnetic, and superconducting behaviors of the system [3,14,15]. Similarly, pressure-induced superconductivity was also reported for $CaFe_2As_2$ and $SrFe_2As_2$, in which Ca and Sr ions are much smaller cations occupying the charge reservoir layers [16–19]. At ambient pressure, the parent $SrFe_2As_2$ compound exhibits the SDW transition at 205 K [20], whereas the superconductivity appears only when suppressing the SDW transition at high pressure [21].

*Corresponding author: jiansun@nju.edu.cn
†Corresponding author: afu@jsg.utexas.edu

It has also been shown that high pressure can cause the tetragonal (T) phase in $SrFe_2As_2$ to transform into a collapsed tetragonal (CT) phase [22]. The complex interactions between structural, magnetic, and superconducting parameters indicate that the lattice dynamics can play a key role in the origin of superconductivity in the pnictides. Knowledge of the partial PDOS of iron in pnictides can provide valuable information about the lattice dynamics and vibrational, thermodynamic, and elastic properties of the system. Previous nuclear resonant inelastic x-ray scattering (NRIXS) experiments performed on both the parent and doped $Ba(Fe_{1-x}Co_x)_2As_2$ iron pnictides have provided information about the partial PDOS of iron and revealed pressure-induced phonon stiffing at 4 GPa and 300 K. A temperature-induced discontinuity of the phonon frequencies was also reported to occur across the magnetic and structural phase transition at 130 K under ambient pressure [23]. The change of the phonon properties around these transitions suggested a close correlation between the partial PDOS of iron and the magnetic and structural transitions in the sample that were driven by applied low temperature and high pressure. Therefore, studying the PDOS and lattice and hyperfine parameters of the pnictide system under controlled hydrostatic pressure conditions is helpful in understanding the structural and magnetic transitions, as well as the formation of superconductivity in the iron pnictide system. In this study, we have investigated the pressure effect on the iron PDOS in a single-crystal $SrFe_2As_2$ enriched in ^{57}Fe isotope using NRIXS and synchrotron x-ray diffraction (XRD) in a high-pressure diamond anvil cell (DAC). Our results show that applied pressure induces an abrupt phonon stiffing in certain vibrational modes across the isostructural T-CT transition. Together with the lattice parameters derived from XRD studies and first-principles theoretical calculations, the phonon stiffing can be associated with the dramatic decrease in the axial c/a ratio, where the elastic constants such as the mean force constant also experience dramatic increase across the transition.

II. EXPERIMENTAL DETAILS

Single-crystal $SrFe_2As_2$ samples with 20 at.% ^{57}Fe enrichment were grown using the FeAs self-flux method [24]. XRD measurements of the sample at ambient conditions showed that the crystal exhibits a tetragonal structure (space group: $I4/mmm$) with $a = 3.925\,6(2)$ Å and $c = 12.379(1)$ Å, consistent with a previous report [25]. A single-crystal sample measuring 25 μm thick and 80 μm in length was loaded into a threefold panoramic DAC with a Be gasket having Ne as the pressure medium and ruby spheres as the pressure calibrant. One crystal was loaded into the DAC with its crystallographic c axis parallel to the compressional axis of the DAC to allow for out-of-plane (OP) NRIXS measurements, while another crystal was loaded into the DAC having its c axis perpendicular to the compression axis for in-plane (IP) NRIXS measurements.

NRIXS experiments were conducted at Sector 3 of the Advanced Photon Source (APS), Argonne National Laboratory (ANL) with an energy resolution of 1 meV and an x-ray beam size of approximately 10 μm in diameter (FWHM). Energy spectra were obtained by tuning the incident x-ray energy (±70 meV) around the nuclear transition energy of 14.412 5 keV, and the Fe K-fluorescence radiation that was emitted with a time delay relative to the incident x-ray pulse was collected by three avalanche photodiode detectors. Our experimental NRIXS method is the same as that used in previous NRIXS studies of $BaFe_2As_2$ and $Ba(Fe_{1-x}Co_x)_2As_2$ [23]. OP measurements were performed with the incident x-ray beam along the c axis of the single crystal, whereas the IP measurements were performed with the incident x-ray beam parallels to the ab basal plane of the crystal. In both OP and IP measurements, the scattered NRIXS signals were measured through the Be gasket. These single-crystal NRIXS measurements from the OP and IP spectra permit us to decipher the evolution of the PDOS along two distinct orientations of the crystal across the collapsed tetragonal transition at high pressures and room temperature. The collection time for each energy spectrum was approximately 8–12 h, and 8–10 spectra at a given pressure were co-added with a maximum phonon intensity of 100–150 counts to allow for sufficient data quality for further analyses. Pressures of the NRIXS experiments were determined from the ruby spheres loaded in the sample chamber, while pressure uncertainties were calculated from measured pressures before and after the experiments at each given pressure step. The measured spectra consisted of an intense elastic peak in the center and a series of sidebands from lower-energy and higher-energy regions. After removing the elastic peak, the measured energy spectra were analyzed using the PHOENIX software using a quasiharmonic model to derive the PDOS, as well as elastic, vibrational, and thermodynamic parameters of the sample [26].

X-ray diffraction experiments were carried out using an incident x-ray wavelength of 0.413 2 Å and a beam size of 20 μm (FWHM) at the 16-BMD beamline of the HPCAT, APS, ANL. A single-crystal sample measuring 50 μm in diameter and 20 μm in thickness was loaded into a symmetric DAC having Ne as the pressure medium and ruby spheres as the pressure calibrant. During the XRD measurements, the crystal in the DAC was rotated at ±2° continuously about the vertical axis of the DAC holder to optimize for the collection of the zone diffraction patterns. Refinements of the lattice parameters of the sample were performed using the LeBail method in the GSAS software package [27].

III. EXPERIMENTAL RESULTS

NRIXS spectra of the single-crystal $SrFe_2As_2$ have been measured up to 15.6 GPa for the out-of-plane orientation and up to 14.5 GPa for the in-plane orientation, respectively (Fig. 1). Analysis of the measured energy spectra and the derived PDOS spectra at ambient conditions shows some prominent spectral features in the low (∼0−20 meV), intermediate (∼20−30 meV), and high-energy (∼ > 30 meV) regions (Fig. 1). The low-energy spectral region consists of three major vibrational bands centered around 9, 14, and 17 meV in which the very-low-energy portion below the band at 9 meV can be attributed to the acoustic phonons. The intermediate- and high-energy regions include two vibrational bands located at around 24 and 31 meV, respectively. The out-of-plane spectra exhibit distinct spectral features in the low-energy region from that in the in-plane spectra (Fig. 1), indicating that the

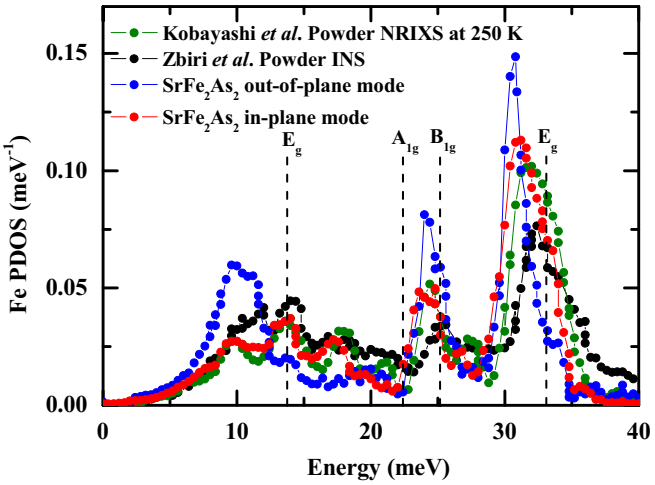

FIG. 1. Representative partial phonon density of state (PDOS) of iron in single-crystal $SrFe_2As_2$ at ambient conditions. Red dots and line: out-of-plane spectra; Blue dots and line: in-plane spectra. The vertical dotted lines represent previously reported frequencies (energies) of the Raman modes from the same compound [30]. Literature PDOS results for powder $SrFe_2As_2$ samples obtained by inelastic neutron scattering at ambient conditions (black line) [28] and by NRIXS at 250 K and ambient pressure (olive line) [29] are also plotted for comparison.

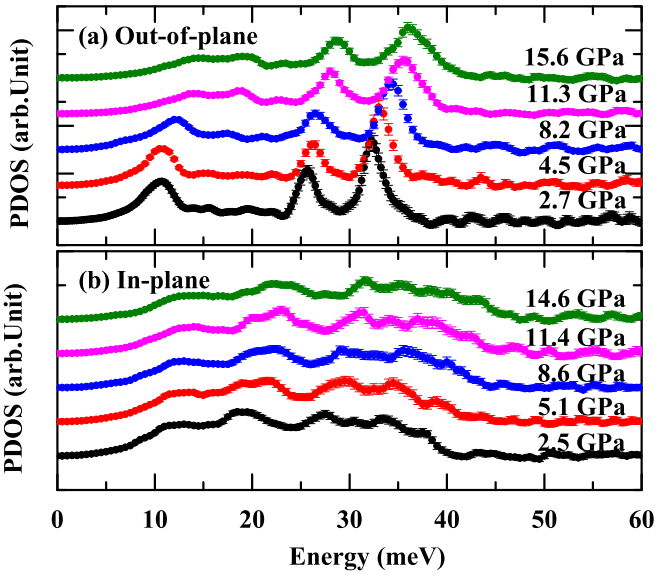

FIG. 2. Representative PDOS spectra of iron in single-crystal $SrFe_2As_2$ measured by NRIXS at high pressures. (a) Out-of-plane spectra measured with the incident x-ray beam along the c axis of the crystal. (b) In-plane spectra with the beam parallel to the ab basal plane. The error bars equal to the symbols suggest very small uncertainties of PDOS. The spectra show a rapid mode stiffening as well as an obvious widening in the region below 20 meV with the pressure increasing from 8 to 11 GPa.

acoustic phonons from the iron lattice displacement in these orientations are very different. Overall, the spectral features of our PDOS spectra are consistent with previous results by neutron inelastic scattering and NRIXS measurements using powder samples at ambient conditions [28,29], although our spectra definitely show many more distinct features due to the use of the preoriented single-crystal sample. Comparison of the Fe PDOS spectra with previously reported Raman spectra of $SrFe_2As_2$ allows us to identify the phonon bands of the B_{1g} mode, which represents the relative vibration of Fe atoms along the c axis at approximately 24 meV, and the E_g mode at around 13 and 31 meV, which represent the two types of relative vibration between Fe and As atoms in the ab plane, respectively [30].

Pressure-dependent PDOS spectra of the single-crystal $SrFe_2As_2$ at room temperature are shown in Fig. 2 for both OP and IP orientations. The spectral features from the OP bands are much more prominent than the IP spectral features. These spectral features are overall in agreement with a previous Raman study of $SrFe_2As_2$ in which the Raman active phonons taken from ac/bc planes are much clearer than those taken from the ab basal plane [30].

The PDOS spectra bands move gradually toward higher energy with increasing pressure up to approximately 8 GPa, corresponding to a normal compression-induced phonon stiffening behavior. However, significant changes in the spectral features occur at pressures from 8.2 to 11.3 GPa [Fig. 2(a)], including the rapid mode stiffening and apparent spectral widening. The pressure-induced spectral changes appear to become more gradual at pressures above 12 GPa. The sharp increase in phonon energy from 8 to 11 GPa indicates that a possible structural transition occurred in this pressure range.

Modeling the experimentally measured energy spectra using the PHOENIX program allows us to derive vibrational, elastic, and thermodynamic parameters of the iron contribution to the lattice dynamics of the $SrFe_2As_2$ lattice as a function of pressure (Fig. 3). We note that although the derived PDOS and physical properties represent only the iron vibrational contributions in the structure, detailed lattice dynamics of the whole sample can still be understood as iron atoms would intrinsically interact with surrounding Sr and As atoms in the lattice, thus providing detailed information about the lattice dynamics of the system at high pressures. Specifically, the Lamb-Mössbauer factor (f_{LM}) represents the probability for recoilless absorption, or the ratio of elastic to total incoherent scattering in NRIXS experiments, which contains information about lattice dynamics and, in turn, depends strongly on the binding of the resonant nuclei in the lattice. The mean force constant reflects the average strength of chemical bonds in the lattice. Thus the derived Lamb-Mössbauer factor (f_{LM}) and mean force constant from the OP and IP orientations can be correlated with the detailed structural parameters along the c axis and ab basal plane.

The f_{LM} and mean force constant derived from both OP and IP orientations gradually increases with increasing pressure up to 8 GPa, indicating an enhanced binding of the resonant nuclei and the chemical bond strength (Fig. 3). At pressures above 8 GPa, however, both the f_{LM} and mean force constant from the OP orientation show a sudden increase from 8.2 to 11.3 GPa, followed by a platform above 12 GPa. The jump is consistent with observations made for the sudden stiffening of the lattice constants along the c axis of $SrFe_2As_2$ based on XRD measurements (Fig. 4; see further discussions below).

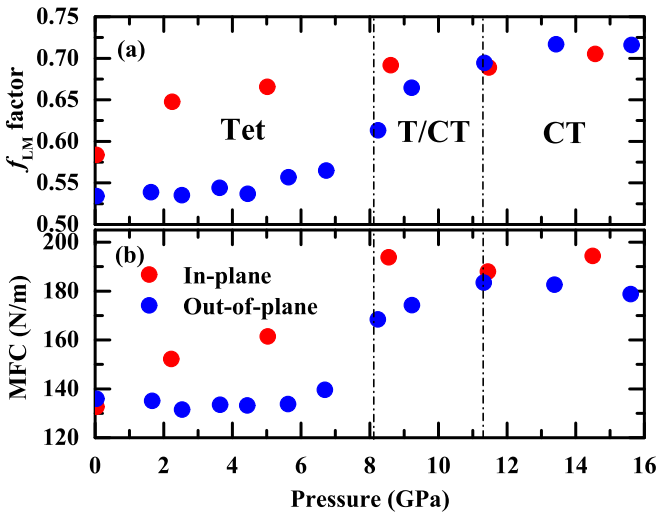

FIG. 3. Derived vibrational and elastic parameters of the single-crystal $SrFe_2As_2$ from the in-plane and out-of-plane PDOS spectra as a function of pressure. (a) Lamb-Mössbauer factor (f_{LM}); (b) mean force constant (MFC). Both the f_{LM} and mean force constant show a sudden jump at 8.2 GPa and experience a rapid increase from 8.2 to 11.3 GPa. Vertical dashed lines are used to separate tetragonal, tetragonal and collapsed tetragonal, and collapsed tetragonal phases. (See Fig. 4 for details.)

On the other hand, for the IP mode, both the f_{LM} and mean force constant rise to maximum values at around 8.6 GPa and then show an abnormal decrease when the pressure increases to 11.4 GPa, suggesting an extended lattice in the ab plane of $SrFe_2As_2$ in the pressure region from 8.6 to 11.4 GPa. The concurrent sudden stiffening along the c axis and abnormal expanding in the ab plane of the lattice of $SrFe_2As_2$ further suggest the occurrence of the structural and/or electronic transition(s) between 8 and 11 GPa.

We have also measured and refined the XRD patterns of the single-crystal $SrFe_2As_2$ in order to understand the correlation between lattice parameters and PDOS. The derived lattice constants, a and c, as a function of pressure are presented in Figs. 4(a) and 4(b). Below 8 GPa, both a and c lattice parameters monotonically decrease with increasing pressure. However, the a axis expands anomalously at pressures above 8 GPa, whereas the c axis shows a rather rapid decrease. The c/a axial ratio also reduces at pressures between 8 and 11 GPa [Fig. 4(c)]. At pressures between 11 and 16 GPa, the axial incompressibility of the crystal appears to become normal with a near constant c/a ratio of 2.65. Here we have analyzed the linear compressibility along the a and c axis according to the extended Eulerian finite-strain equation of state [31]. The modeled linear incompressibilities along the a and c directions are 256.6 (±5.9) and 30.3 (±0.2) GPa, respectively, below 8 GPa and 367.2 (±47.7) and 142.2 (±19.6) GPa, respectively, above 11 GPa. These results show an extremely anisotropic compressional behavior along the a and c axes, in which the c axis is much more compressible than the a axis. Previous high-pressure studies in powder $SrFe_2As_2$ and $BaFe_2Aa_2$ by Uhoya *et al.* [22,32] have revealed an abnormal increase of the a axis and a rapid decrease of the c axis with compression that were found to be associated with the T–CT isostructural transition. Our measured lattice parameters here are thus consistent with the occurrence of the T-CT transition

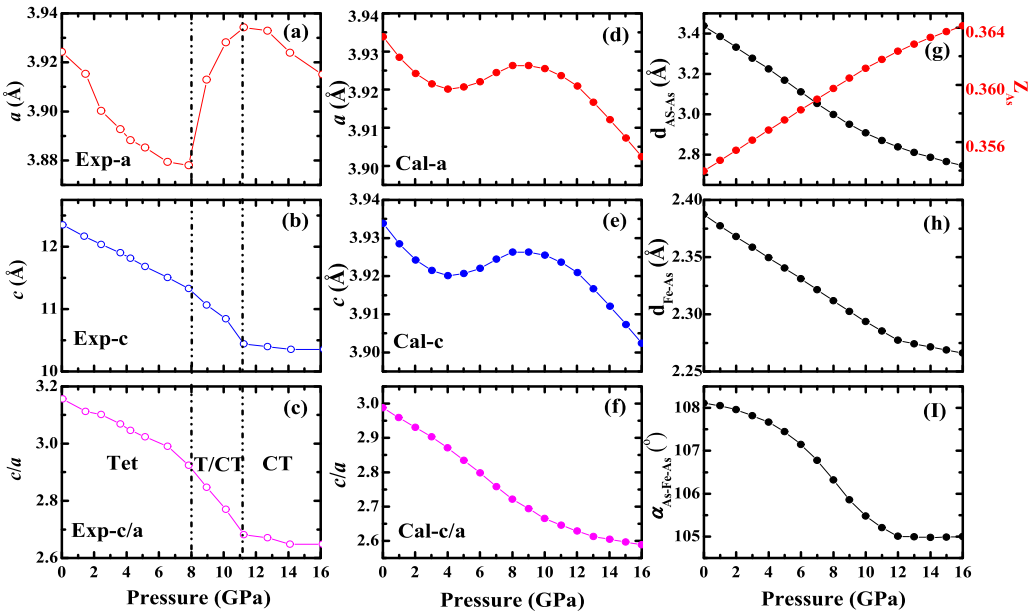

FIG. 4. Experimental (open circle) (a)–(c) and theoretically calculated (solid circle) (d)–(f) lattice parameters a, c and axial ratio c/a of the single-crystal $SrFe_2As_2$ as a function of pressure. Vertical dotted lines indicate tetragonal (T), two-phase coexistence (T/CT), and collapsed tetragonal (CT) phase regions. The abnormal expansion of a and rapid decrease of c between 8 and 11 GPa highlight the occurrence of T-CT phase transition. The calculated results give a similar change tendency and confirm the phase transition observed in the XRD experiments. Theoretically calculated As-As bond length and Z_{As} (g), Fe-As bond length (h), and As-Fe-As bond angles (i) as a function of pressure. These results suggest a relatively less decrease of the bond lengths and bond angles with the increasing pressure above 11 GPa as a result of As-As interactions strengthening.

in $SrFe_2As_2$ at high pressures. The T-CT phase transition starts at ~8 GPa, where the lattice parameters abnormally change. At approximately 11 GPa, the $SrFe_2As_2$ transforms completely to the CT structure with the same space group of $I4/mmm$ but with a larger a and smaller c lattice parameter. This collapsed tetragonal isostructural transition has also been reported for other "122" pnictide superconductors [33,34]. It should be noted that the T-CT phase transition observed at 8–11 GPa in our study is slightly higher than the pressure range of 5–10 GPa in a previous study on powder $SrFe_2As_2$ under nonhydrostatic conditions. [22] This difference in the transition pressure can be attributed to the presence of the uniaxial stress in the sample chamber with the different pressure medium used. Such a nonhydrostatic pressure-induced transition has also been observed in $BaFe_2As_2$ in which the starting transition pressure is 17 GPa under nonhydrostatic conditions [32] and 22 GPa under hydrostatic conditions [35], respectively.

IV. THEORETICAL CALCULATIONS

In order to help decipher the underlying physics for the changes in the lattice parameters and PDOS across the T-CT transition in $SrFe_2As_2$ at high pressure, first-principles calculations were carried out using the VASP code [36], projector augmented wave pseudopotentials with the Perdew-Burke-Ernzerhof generalized gradient approximation density functional [37]. The geometry optimization was performed over a $9 \times 9 \times 12$ k-point grid, with cutoff of 500 eV for the wave functions. The phonon spectra calculations were performed through the finite displacement method implemented in the PHONOPY code [38], with a $2 \times 2 \times 2$ supercell for force constant set calculations.

The lattice parameters and atomic positions of $SrFe_2As_2$ at high pressures were obtained from nonspin polarized geometry optimization, as shown in Figs. 4(d)–4(f), which show similar trends as the experimentally measured results. Specifically, the abnormal expansion of the lattice parameter a and the change of the slope of c/a ratio upon pressure are shown to be associated with the electronic collapsing across the T-CT transition [35,39]. The variations of As-As and Fe-As bond length as well as As-Fe-As bond angles after relaxation, which have been also calculated and presented in Figs. 4(g)–4(i), are associated with a significant decrease in the height of the FeAs and As-Sr-As planes below transition pressure. This reduction is not as apparent at higher pressure and can be attributed to pressure-induced strengthening of the As-As interactions [40,41,42]. The calculated phonon spectra of $SrFe_2As_2$ at 16 GPa are plotted in Fig. 5, which shows the dynamical stabilities of the CT phase of $SrFe_2As_2$ under high pressure and confirms the T-CT phase transition. The structural stability could also be ascribed to the enhanced As-As interactions under high pressure [43].

The evolution of Fe out-of-plane spectra under high pressure, shown in Fig. 5(b), agrees with the experiments reasonably well. To figure out the vibrational mode compound of each peak, we carried out Γ-point phonon calculations. The vibrational modes related to Fe atoms and the evolution of frequency with pressure are shown in Fig. 5(c). There are eight irreducible representations of the optical phonons in $SrFe_2As_2$

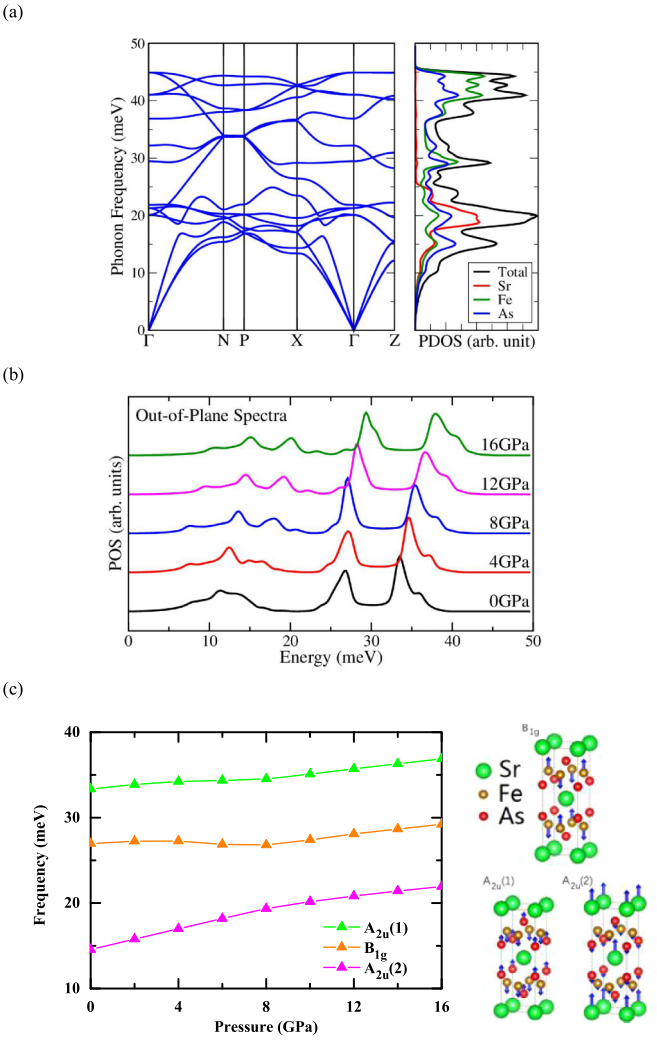

FIG. 5. Theoretically calculated (a) phonon spectra and phonon DOS of $SrFe_2As_2$ at 16 GPa, which shows the CT structure is dynamically stable at high pressure. (b) Partial phonon DOS of Fe in $SrFe_2As_2$ at high pressures projected on the out-of-plane direction. (c) The vibrational modes at Γ point associated with the Fe out-of-plane vibration. The pressure dependence of these modes has a similar evolution as the measured out-of-plane modes from experiments. The intermediate-frequency B_{1g} mode at around 20–30 meV indicates a nonmonotonic variation with pressure.

at the Γ point for the D_{4h} ($4/mmm$) group:

$$\Gamma_{\text{optic}} = A_{1g} + 2A_{2u} + B_{1g} + 2E_g + 2E_u.$$

The spectra in the low-energy spectral region (10–20 meV) emerge as two bands, which are contributed by the acoustic modes and the optical $A_{2u}(2)$ mode, respectively. These two bands separate from each other with increasing pressure, which agrees with the widening of spectra observed in our experiment. In the intermediate (~20−30 meV) region, the peak corresponding to the B_{1g} mode indicates a nonmonotonic variation in frequency, consistent with the experimental result shown in Fig. 2(a). The vibrational phonon B_{1g} stiffens at the pressure of 0 ~ 4 GPa, then softens at around 7 GPa, and finally stiffens rapidly at pressure above 8 GPa, exhibiting a similar trend to the evolution of the a axis in the lattice.

As shown in Fig. 5(c), the B_{1g} mode represents the Fe-Fe asymmetric off-plane vibration along the c axis, and Fe-Fe distance ($= a/\sqrt{2}$) may significantly influence the vibrational frequency of this mode. The $A_{2u}(1)$ mode in the high-energy ($\sim>30$ meV) region, representing the Fe-As asymmetric off-plane vibration, shows a rapid stiffening at pressure above 8 GPa, which is in agreement with the increasing of experimental out-of-plane mean force constant during T-CT transition.

Based on these high-pressure NRIXS and XRD results of the single-crystal $SrFe_2As_2$ as well as theoretical calculations for the structural parameters, phonon dispersions, and PDOS, here we address how phononic and structural properties of the sample are affected by the pressure-induced T-CT transition. Our observed drastic changes in the PDOS between 8 and 11 GPa can be directly associated with the occurrence of the collapsed tetragonal transition. Thus the evolution of the derived f_{LM} and mean force constant in OP and IP modes can be associated to the abnormal change of the lattice constants of a and c across the T-CT transition. Between 8 and 11 GPa, the rapid decrease of c with the increasing pressure indicates a quick shortening of atomic spacing along the c-axis direction; therefore, the phonon mode B_{1g}, which represents the Fe-Fe stretching vibration along the c axis, shows a rapid stiffening in the OP mode. Correspondingly, the derived f_{LM} and mean force constant in OP mode shows a rapid increase in the pressure region. On the contrary, the increase of the lattice parameter a across the T-CT transition induces an expansion in the ab plane and an abnormal decrease of f_{LM} and mean force constant in IP mode from 8.6 to 11.4 GPa (Fig. 3).

V. CONCLUSION

The pressure dependence of the partial phonon density of states in the single-crystal $SrFe_2As_2$ has been studied by the high-energy resolution ^{57}Fe NRIXS together with x-ray diffraction under hydrostatic conditions. Our x-ray diffraction studies reveal anomalous changes of the lattice parameters between 8 and 11 GPa with an abnormal change in a and rapid decrease in c, which can be associated to the isostructural phase transition from the tetragonal to the collapsed tetragonal phase. The Fe partial PDOS of the SrF_2As_2 were found to be drastically affected by the phase transition such that a stiffening of the vibrational modes was observed in both the OP and IP polarized modes under high pressure. Accompanied with the phase transition and mode stiffening, the elastic and vibrational parameters, such as Lamb-Mössbauer factor and mean force constant, show drastic change across the T-CT transition between 8 and 11 GPa. These changes in PDOS, f_{LM}, and mean force constant can be associated with the anomalous changes of the lattice parameters, a and c, as a result of the T-CT phase transition under high pressure. Our results here can be used to help understand the evolution of phononic and structural properties across the T-CT phase transition in $SrFe_2As_2$ at high pressures.

ACKNOWLEDGMENTS

We acknowledge sector 3 (XSD) and HPCAT, APS, and ANL for the use of the synchrotron facilities. HPCAT is supported by CIW, CDAC, UNLV, and LLNL through funding from DOE-NNSA, DOE-BES, and NFS. APS is supported by DOE-BES under Contract No. DE-AC02-06CH11357. Work at the Institute of Physics, Chinese Academy of Sciences, is supported by NSF and MOST of China through research projects. Work at Nanjing University is supported by the National Key Projects for Research & Development of China (Grant No. 2016YFA0300404), 973 project (Grant No. 2015CB921202), the National Natural Science Foundation of China (Grants No. 51372112 and No. 11574133), NSF Jiangsu province (No. BK20150012), and the Fundamental Research Funds for the Central Universities and Special Program for Applied Research on Super Computation of the NSFC-Guangdong Joint Fund (the second phase). This research was partially supported by COMPRES, the Consortium for Materials Properties Research in Earth Sciences under NSF Cooperative Agreement EAR 1606856. Part of the calculations were performed on the supercomputer in the High Performance Computing Center of Nanjing University.

[1] Y. Kamihara, T. Watanabe, M. Hirano, and H. Hosono, Iron-based layered superconductor $La[O_{1-x}F_x]FeAs$ ($x = 0.05-0.12$) with $T_c = 26$ K, J. Am. Chem. Soc. **130**, 3296 (2008).

[2] K. Ishida, Y. Nakai, and H. Hosono, To what extent iron-pnictide new superconductors have been clarified: A progress report, J. Phys. Soc. Jpn. **78**, 062001 (2009).

[3] J. Paglione and R. L. Greene, High-temperature superconductivity in iron-based materials, Nat. Phys. **6**, 645 (2010).

[4] C. de la Cruz, Q. Huang, J. W. Lynn, J. Li, W. Ratcliff, II, J. L. Zarestky, H. A. Mook, G. F. Chen, J. L. Luo, N. L. Wang, and P. Dai, Magnetic order close to superconductivity in the iron-based layered $LaO_{1-x}F_xFeAs$ systems, Nature (London) **453**, 899 (2008).

[5] M. Rotter, M. Tegel, D. Johrendt, I. Schellenberg, W. Hermes, and R. Pottgen, Spin-density-wave anomaly at 140 K in the ternary iron arsenide $BaFe_2As_2$, Phys. Rev. B **78**, 020503(R) (2008).

[6] G. F. Chen, W. Z. Hu, J. L. Luo, and N. L. Wang, Multiple Phase Transitions in Single-Crystalline $Na_{1-\delta}FeAs$, Phys. Rev. Lett. **102**, 227004 (2009).

[7] G. R. Stewart, Superconductivity in iron compounds, Rev. Mod. Phys. **83**, 1589 (2011).

[8] L. Boeri, O. V. Dolgov, and A. A. Golubov, Is $LaFeAsO_{1-x}F_x$ an Electron-Phonon Superconductor?, Phys. Rev. Lett. **101**, 026403 (2008).

[9] M. Zbiri, H. Schober, M. R. Johnson, S. Rols, R. Mittal, Y. Su, M. Rotter, and D. Johrendt, *Ab initio* lattice dynamics simulations and inelastic neutron scattering spectra for studying phonons in $BaFe_2As_2$: Effect of structural phase transition, structural relaxation, and magnetic ordering, Phys. Rev. B **79**, 064511 (2009).

[10] D. Reznik, K. Lokshin, D. C. Mitchell, D. Parshall, W. Dmowski, D. Lamago, R. Heid, K.-P. Bohnen, A. S. Sefat, M. A. McGuire *et al.*, Phonons in doped and undoped $BaFe_2As_2$ investigated by inelastic x-ray scattering, Phys. Rev. B **80**, 214534 (2009).

[11] R. H. Liu, T. Wu, G. Wu, H. Chen, X. F. Wang, Y. L. Xie, J. J. Ying, Y. J. Yan, Q. J. Li, B. C. Shi *et al.*, A large iron isotope effect in $SmFeAsO_{1-x}F_x$ and $Ba_{1-x}K_xFe_2As_2$, Nature (London) **459**, 64 (2009).

[12] R. Khasanov, M. Bendele, K. Conder, H. Keller, E. Pomjakushina, and V. Pomjakushin, Iron isotope effect on the superconducting transition temperature and the crystal structure of $FeSe_{1-x}$, New J. Phys. **12**, 073024 (2010).

[13] A. S. Sefat, Pressure effects on two superconducting iron-based families, Rep. Prog. Phys. **74**, 124502 (2011).

[14] W. J. Duncan, O. P. Welzel, C. Harrison, X. F. Wang, X. H. Chen, F. M. Grosche, and P. G. Niklowitz, High pressure study of $BaFe_2As_2$—The role of hydrostaticity and uniaxial stress, J. Phys.: Condens. Matter **22**, 052201 (2010).

[15] T. Yamazaki, N. Takeshita, R. Kobayashi, H. Fukazawa, Y. Kohori, K. Kihou, C. H. Lee, H. Kito, A. Iyo, and H. Eisaki, Appearance of pressure-induced superconductivity in $BaFe_2As_2$ under hydrostatic conditions and its extremely high sensitivity to uniaxial stress, Phys. Rev. B **81**, 224511 (2010).

[16] T. Park, E. Park, H. Lee, T. Klimczuk, E. D. Bauer, F. Ronning, and J. D. Thompson, Pressure-induced superconductivity in $CaFe_2As_2$, J. Phys.: Condens. Matter **20**, 322204 (2008).

[17] M. S. Torikachvili, S. L. Bud'ko, N. Ni, and P. C. Canfield, Pressure Induced Superconductivity in $CaFe_2As_2$, Phys. Rev. Lett. **101**, 057006 (2008).

[18] H. Kotegawa, T. Kawazoe, H. Sugawara, K. Murata, and H. Tou, Effect of uniaxial stress for pressure-induced superconductor $SrFe_2As_2$, J. Phys. Soc. Jpn. **78**, 083702 (2009).

[19] H. Kotegawa, H. Sugawara, and H. Tou, Abrupt emergence of pressure-induced superconductivity of 34 K in $SrFe_2As_2$: A resistivity study under pressure, J. Phys. Soc. Jpn. **78**, 013709 (2009).

[20] A. Jesche, N. Caroca-Canales, H. Rosner, H. Borrmann, A. Ormeci, D. Kasinathan, H. H. Klauss, H. Luetkens, R. Khasanov, A. Amato *et al.*, Strong coupling between magnetic and structural order parameters in $SrFe_2As_2$, Phys. Rev. B **78**, 180504(R) (2008).

[21] K. Igawa, H. Okada, H. Takahashi, S. Matsuishi, Y. Kamihara, M.Hirano, H. Hosono, K. Matsubayashi, and Y. Uwatoko, Pressure-induced superconductivity in iron pnictide compound $SrFe_2As_2$, J. Phys. Soc. Jpn. **78**, 025001 (2009).

[22] W. O. Uhoya, J. M. Montgomery, G. M. Tsoi, Y. K. Vohra, M. A. McGuire, A. S. Sefat, B. C. Sales, and S. T. Weir, Phase transition and superconductivity of $SrFe_2As_2$ under high pressure, J. Phys.: Condens. Matter **23**, 122201 (2011).

[23] O. Delaire, M. S. Lucas, A. M. dos Santos, A. Subedi, A. S. Sefat, M. A. McGuire, L. Mauget, J. A. Muñoz, C. A. Tulk, Y. Xiao *et al.*, Temperature and pressure dependence of the Fe-specific phonon density of states in $Ba(Fe_{1-x}Co_x)_2As_2$, Phys. Rev. B **81**, 094504 (2010).

[24] K. Zhao, Q. Q. Liu, X. C. Wang, Z. Deng, Y. X. Lv, J. L. Zhu, F. Y. Li, and C. Q. Jin, Superconductivity above 33 K in $(Ca_{1-x}Na_x)Fe_2As_2$, J. Phys.: Condens. Matter **22**, 222203 (2010).

[25] M. Tegel, M. Rotter, V. Weib, F. M. Schappacher, R. Pottgen, and D. Johrendt, Structural and magnetic phase transitions in the ternary iron arsenides $SrFe_2As_2$ and $EuFe_2As_2$, J. Phys.: Condens. Matter **20**, 452201 (2008).

[26] W. Sturhahn, CONUSS and PHOENIX: Evaluation of nuclear resonant scattering data, Hyperfine Interact. **125**, 149 (2000).

[27] A. C. Larson and R. B. Von Dreele, GSAS—General structure analysis system, Los Alamos National Laboratory Report No. LAUR 86-748, 2004 (unpublished).

[28] M. Zbiri, R. Mittal, S. Rols, Y. Su, Y. Xiao, H. Schober, S. L. Chaplot, M. R. Johnson, T. Chatterji, Y. Inoue *et al.*, Magnetic lattice dynamics of the oxygen-free FeAs pnictides: How sensitive are phonons to magnetic ordering?, J. Phys.: Condens. Matter **22**, 315701 (2010).

[29] H. Kobayashi and S. Ikeda, Orthorhombic fluctuations in tetragonal AFe_2As_2 (A = Sr and Eu), Phys. Rev. B **84**, 184304 (2011).

[30] A. P. Litvinchuk, V. G. Hadjiev, M. N. Iliev, B. Lv, A. M. Guloy, and C. W. Chu, Raman-scattering study of $K_xSr_{1-x}Fe_2As_2$ (x = 0.0,0.4), Phys. Rev. B **78**, 060503(R) (2008).

[31] H. Liu, W. A. Caldwell, L. R. Benedetti, W. Panero, and R. Jeanloz, Static compression of a-Fe_2O_3: Linear incompressibility of lattice parameters and high-pressure transformations, Phys. Chem. Miner. **30**, 582 (2003).

[32] W. Uhoya, A. Stemshorn, G. Tsoi, Y. K. Vohra, A. S. Sefat, and B. C. Sales, Collapsed tetragonal phase and superconductivity of $BaFe_2As_2$ under high pressure, Phys. Rev. B **82**, 144118 (2010).

[33] W. Uhoya, G. Tsoi, Y. K. Vohra, M. A. McGuire, A. S. Sefat, B. C. Sales, D. Mandrus, and S. T. Weir, Anomalous compressibility effects and superconductivity of $EuFe_2As_2$ under high pressures, J. Phys.: Condens. Matter **22**, 292202 (2010).

[34] A. I. Goldman, A. Kreyssig, K. Prokes, D. K. Pratt, D. N. Argyriou, J. W. Lynn, S. Nandi, S. A. J. Kimber, Y. Chen, Y. B. Lee *et al.*, Lattice collapse and quenching of magnetism in $CaFe_2As_2$ under pressure: A single-crystal neutron and x-ray diffraction investigation, Phys. Rev. B **79**, 024513 (2009).

[35] R. Mittal, S. K. Mishra, S. L. Chaplot, S. V. Ovsyannikov, E. Greenberg, D. M. Trots, L. Dubrovinsky, Y. Su, Th. Brueckel, S. Matsuishi *et al.*, Ambient- and low-temperature synchrotron X-ray diffraction study of $BaFe_2As_2$ and $CaFe_2As_2$ at high pressures up to 56 GPa, Phys. Rev. B **83**, 054503 (2011).

[36] G. Kresse and J. Furthmüller, Efficiency of ab-initio total energy calculations for metals and semiconductors using a plane-wave basis set, Comput. Mater. Sci. **6**, 15 (1996).

[37] J. P. Perdew, K. Burke, and M. Ernzerhof, Generalized Gradient Approximation Made Simple, Phys. Rev. Lett. **77**, 3865 (1996).

[38] A. Togo, F. Oba, and I. Tanaka, First-principles calculations of the ferroelastic transition between rutile-type and $CaCl_2$-type SiO_2 at high pressures, Phys. Rev. B **78**, 134106 (2008).

[39] M. Aghajani, H. Khosroabadi, and M. Akhavan, Evolution of the electronic structure and structural properties of $BaFe_2As_2$ at the tetragonal-collapsed tetragonal phase transition, Physica C **516**, 36 (2015).

[40] T. Yildirim, Strong Coupling of the Fe-Spin State and the As-As Hybridization in Iron-Pnictide Superconductors from First-Principle Calculations, Phys. Rev. Lett. **102**, 037003 (2009).

[41] J. J. Wu, J. F. Lin, X. C. Wang, Q. Q. Liu, J. L. Zhu, Y. M. Xiao, P. Chow, and C. Q. Jin, Magnetic and structural transitions of $SrFe_2As_2$ at high pressure and low temperature, Sci. Rep. **4**, 3685 (2014).

[42] K. Matsubavashi, N. Katayama, K. Ohgushi, A. Yamada, K. Munakata, T. Matsumoto, and Y. Uwatoko, Intrinsic properties of AFe_2As_2 (A = Ba, Sr) single crystal under highly hysrostatic pressure conditions, J. Phys. Soc. Jpn. **78**, 073706 (2009).

[43] J. J. Wu, J. F. Lin, X. C. Wang, Q. Q. Liu, J. L. Zhu, Y. M. Xiao, P. Chow, and C. Q. Jin, Pressure-decoupled magnetic and structural transitions of the parent compound of iron-based 122 superconductors $BaFe_2As_2$, PNAS **110**, 17263 (2013).